Supplementary Information for

Facile transformation of low cost thiourea into nitrogen-rich graphitic carbon nitride nanocatalyst with high visible light photocatalytic performance

Fan Dong[*a], Yanjuan Sun [a], Liwen Wu [a], Min Fu [a] and Zhongbiao Wu[*b],

[a] College of Environmental and Biological Engineering, Key Laboratory of Catalysis Science and Technology of Chongqing Education Commission, Chongqing Technology and Business University, Chongqing, 400067, China.

[b] Department of Environmental Engineering, Zhejiang University, Hangzhou 310027, China.

[*]To whom correspondence should be addressed.
E-mail: dfctbu@126.com (Fan Dong), zbwu@zju.edu.cn (Zhongbiao Wu)

Experimental Section

Synthesis of g-C_3N_4

All chemicals used in this study were analytical grade and were used without further purification. In a typical synthesis, 10 g of thiourea powder was put into an alumina crucible with a cover, and then heated to 550 ^oC at a heating rate of 15 ^oC /min in a tube furnace for 2 h in air. The released air product during thermal treatment was absorbed by dilute NaOH solution (0.05 M). The resulted final yellow powder (g-C_3N_4-T) was collected for use without further treatment. For comparison, g-C_3N_4 polymer (g-C_3N_4-D) was also prepared by heating dicyandiamide at 550 ^oC for 2 h. C-doped TiO_2 (C-TiO_2) was prepared a hydrothermal approach.[1] The two samples were used as references.

Characterization

The crystal phase was analyzed by X-ray diffraction with Cu Kα radiation (XRD: model D/max RA, Japan). X-ray photoelectron spectroscopy with Al Kα X-rays ($h\nu$=1486.6eV) radiation (XPS: Thermo ESCALAB 250, USA) was used to investigate the surface properties and to probe the total density of the state (DOS) distribution in the valence band. The shift of the binding energy was corrected using the C1s level at 284.8 eV as an internal standard. A scanning electron microscope (SEM, JEOL model JSM-6490, Japan) was used to characterize the morphology of the samples. The morphology and structure were examined by transmission electron microscopy (TEM: JEM-2010, Japan). The UV-vis diffuse reflection spectra were obtained for the dry-pressed disk samples using a Scan UV-vis spectrophotometer (UV-vis DRS: UV-2450, Shimadzu, Japan) equipped with an integrating sphere assembly, using $BaSO_4$ as reflectance sample. The photoluminescence spectra were measured with a fluorescence spectrophotometer (F-7000, Japan) using a Xe lamp as excitation source with optical filters. Nitrogen adsorption-desorption isotherms were obtained on a nitrogen adsorption apparatus (ASAP 2020, USA) with all samples degassed at 150°C prior to measurements.

Evaluation of visible light photocatalytic activity

Photocatalytic activity of g-C_3N_4 polymer for degradation of aqueous Rodamine B (RhB) was evaluated in a quartz glass reactor. 0.05 g of g-C_3N_4 was dispersed in RhB aqueous solution (55 mL, 5 mg/L). The light irradiation system contains a 500 W Xe lamp with a jacket filled with flowing and thermostatted aqueous $NaNO_2$ solution (1 M) between the lamp and the reaction chamber as a filter to block UV light ($\lambda < 400$ nm) and eliminate the temperature effect. Before irradiation, the suspension was allowed to reach equilibrium with continuous stirring for 60 min. The degradation efficiency of RhB was evaluated using the UV-vis absorption spectra to measure the peak value of a

maximum absorption of RhB solution. During the irradiation, 5mL of suspension was continually taken from the reaction cell at given time intervals for subsequent dye concentration analysis after centrifuging. The RhB solution shows a similar pH value at 6.8, which does not affect the light absorption of RhB. The maximum absorption of RhB is at wavelength of 552 nm. The removal ratio (%) can be calculated as η (%) = $(C_0 - C)/C_0 \times 100\%$, where C_0 is the initial concentration of RhB considering RhB adsorption on the catalyst and C is the revised concentration after irradiation.

Table S1. The S_{BET}, pore volume, band gap energy, removal ratio and initial rate constant k of g-C_3N_4-T, g-C_3N_4-D and C-doped TiO_2.

Samples	S_{BET} (m^2/g)	Pore volume (cm^3/g)	Band Gap (eV)	Removal ratio η (%)	k (min^{-1})
g-C_3N_4-T	27.1	0.042	2.46	70.9	0.0031
g-C_3N_4-D	30.4	0.185	2.58	49.3	0.0018
C-doped TiO_2	122.5	0.248	2.90	14.9	0.0003

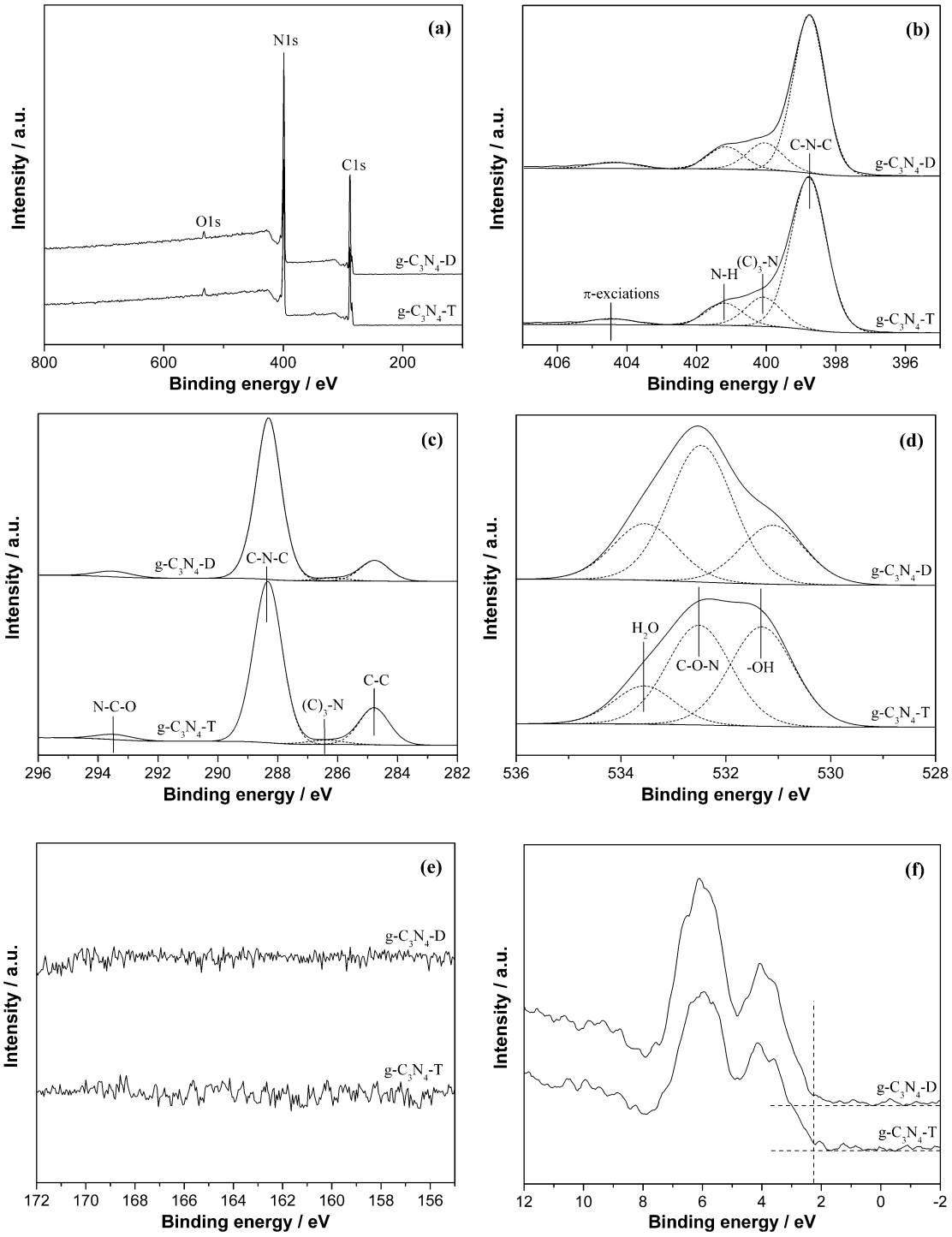

Fig. S1 XPS spectra of g-C_3N_4-T and g-C_3N_4-D, (a) survey (b) N1s (c) C1s, (d) O1s (e) S2p and (f) VB.

Discussions on XPS results in Fig. S1

The XPS measurements were carried out to determine the chemical state of the elements and total density of states distribution (DOS) of the valence band for g-C_3N_4-T and g-C_3N_4-D samples, as shown in Fig. S1. Signals of C, N and O elements are displayed in the spectra survey for the two samples and no peak assigned to S species can be seen for g-C_3N_4-T (Fig. S1a). The N1s region can be fitted into four peaks (Fig. S1b), which can be ascribed to C-N-C (398.8 eV), N-$(C)_3$ (400.1 eV),

N-H groups (401.2 eV) and π-excitations (404.5 eV), respectively.[2,3] The C1s spectra in Fig. S1c shows the deconvoluted four peaks, which can be assigned to adventitious carbon species (284.8 eV), C-$(N)_3$ (286.5 eV), C-N-C (288.3 eV) and N-C-O (293.4 eV), respectively.[3] O1s XPS can be fitted into three peaks (Fig. S1d), which can be assigned to chemisorbed H_2O (533.5 eV), O-C-N (532.4 eV) and hydroxyl (-OH) groups (531.3 eV), respectively.[4] Obviously, the oxygen (O-C-N) contained in the samples comes from the heating treatment in presence of air. No sulfur species are detected on the surface of g-C_3N_4-T by XPS (Fig. S1e). Preliminary results indicate that sulfur in thiourea is released to air in the form of CS_2 during heating treatment. The detailed the formation mechanism of g-C_3N_4 from thiourea is underway. The DOS of valance band (VB) is shown in Fig. S1f. The valence band maximum (VBM) is determined to be 2.2 eV for both samples.

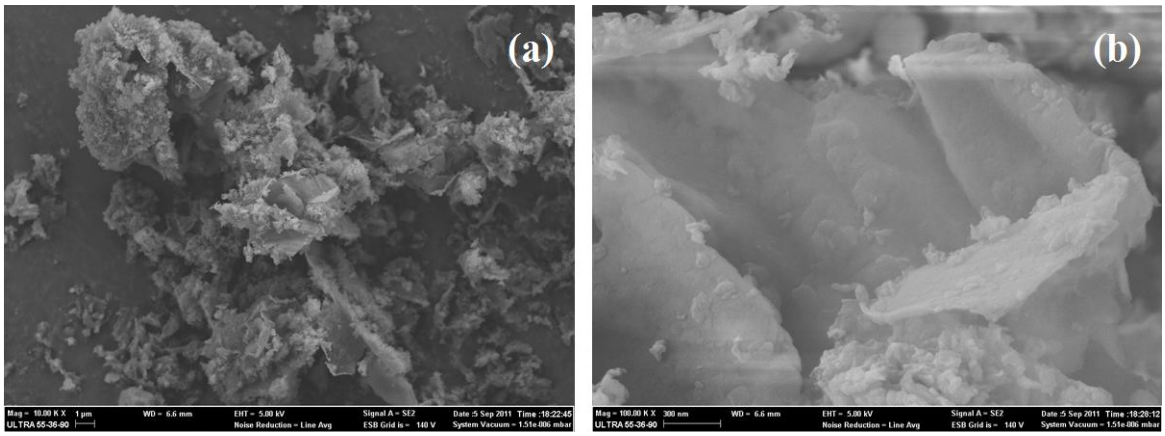

Fig. S2 SEM images of g-C_3N_4-D

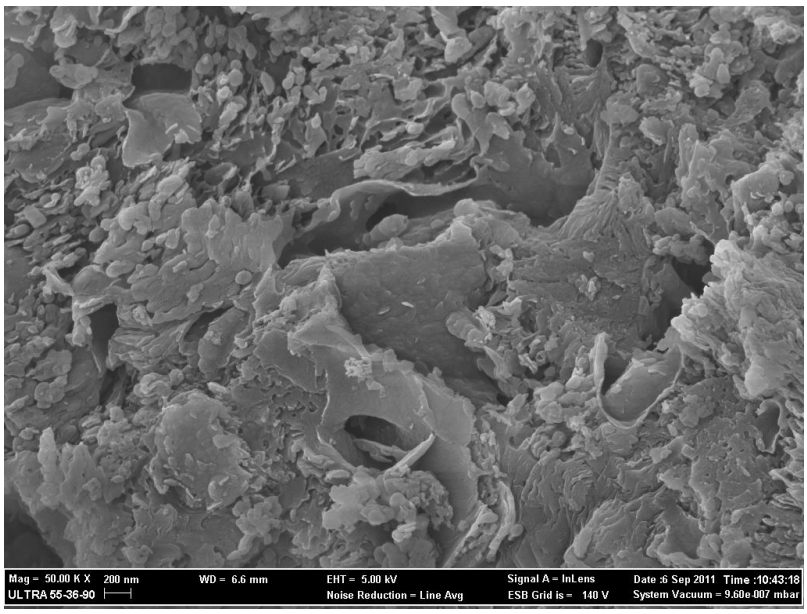

Fig. S3 SEM images of g-C_3N_4-T

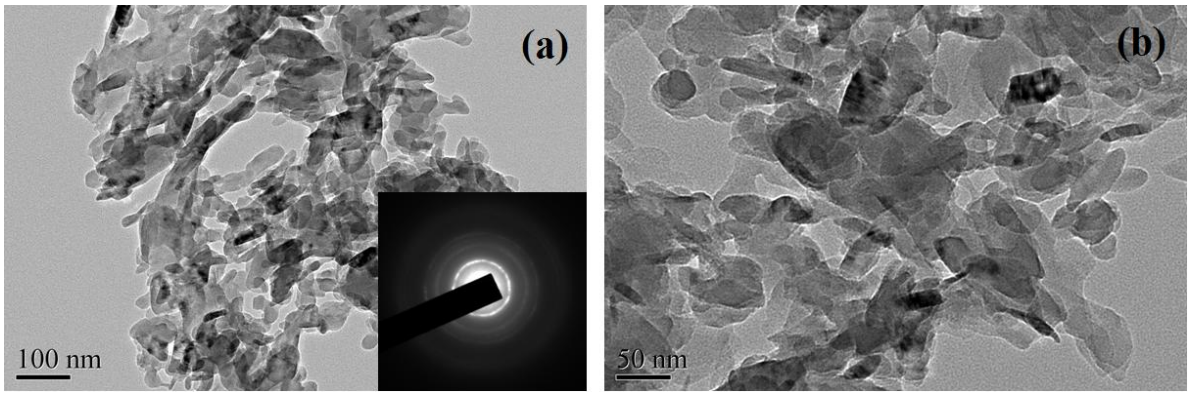

Fig. S4 TEM images of g-C_3N_4-D (a, b), inset in (a) shows SAED image.

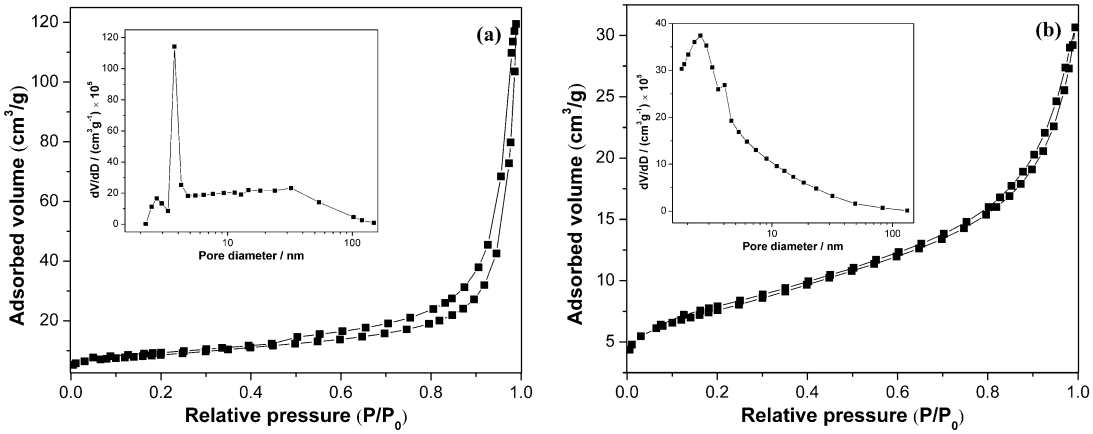

Fig. S5 N_2 adsorption-desorption isotherms of g-C_3N_4-D (a) and g-C_3N_4-T (b), the inset in (a) and (b) shows the corresponding pore-size distribution curves.

Discussions on pore structure in Fig. S5.

Fig. S5 shows the nitrogen adsorption-desorption isotherms and the corresponding curves of the pore size distribution for g-C_3N_4-D and g-C_3N_4-T. The isotherm of g-C_3N_4-D is close to tpye IV, which implies the presence of mesopores.[5] The g-C_3N_4-D (Inset in Fig. S5a) is bimodal with small mesopores (ca. 3.7 nm) and large mesopores (32.3 nm). The aggregation of nanosheets and nanoparticles contributed to the formation of the observed mesopores (Fig. S2). The isotherm of g-C_3N_4-T can be clasifed as tpye II. The pore volume of g-C_3N_4-T is small (Table S1). It can be observed that the g-C_3N_4-T has mesopores of 2.5 and 4.0 nm (Inset in Fig. S5b), which can be ascribed to the interconnected network (Fig. 2a). The BET surface area (S_{BET}) and pore volume of the g-C_3N_4-D are higher than that of the g-C_3N_4-T (Table S1). The mesoporous structure is proved to facilitate the transportation of reactants and products through the interior space due to the interconnected porous network and to favor the harvesting of photo-energy due to multiple

scattering within the porous framework.[6-9]

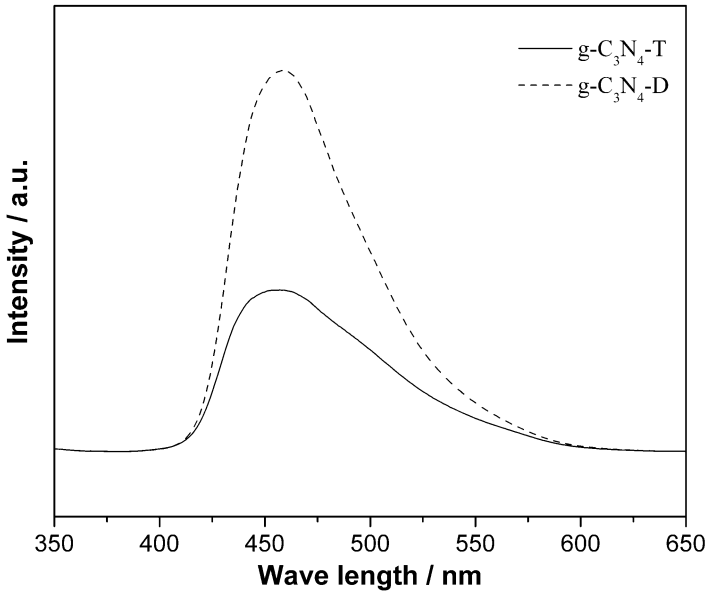

Fig. S6 Room temperature PL spectra of g-C_3N_4-T and g-C_3N_4-D (excitation light source: 335 nm)

References

[1] F. Dong, S. Guo, H. Q. Wang, X. F. Li and Z. B. Wu, *J. Phys. Chem. C*, 2011, **115**, 13285.

[2] X. X. Zou, G. D. Li, Y. N. Wang, J. Zhao, C. Yan, M. Y. Guo, L. Li and J. S. Chen, *Chem. Commun.*, 2011, **47**, 1066.

[3] F. Dong, L. W. Wu, Y. J. Sun, M. Fu, Z. B. Wu and S. C. Lee, *J. Mater. Chem.*, 2011, **21**, 15171.

[4] J. G. Yu, G. H. Wang, B. Cheng and M. H. Zhou, *Appl. Catal. B*, 2007, **69**, 171.

[5] K. S. W. Sing, D. H. Everett, R. A. W. Haul, L. Moscou, R. A. Pierotti, J. Rouquerol and T. Siemieniewska, *Pure Appl. Chem.*, 1985, **57**, 603.

[6] X. X. Yu, J. G. Yu, B. Cheng and M. Jaroniec, *J. Phys. Chem. C*, 2009, **113**, 17527.

[7] H. X. Li, Z. F. Bian, J. Zhu, D. Q. Zhang, G. S. Li, Y. N. Huo, H. Li and Y. F. Lu, *J. Am. Chem. Soc.*, 2007, **129**, 8406.

[8] J. G. Yu, Y. R. Su and B. Cheng, *Adv. Funct. Mater.*, 2007, **17**, 1984.

[9] G. S. Li, D. Q. Zhang, J. C. Yu and M. K. H. Leung, *Environ. Sci. Technol.*, 2010, **44**, 4276.